Solvent-Induced Crystallization of Spherical Micelles Formed by Copolymer Blends

Weihuan Huang, Chunxia Luo, Binyao Li, and Yanchun Han*

State Key Laboratory of Polymer Physics and Chemistry, Changchun Institute of Applied Chemistry, Chinese Academy of Sciences; Graduate School of the Chinese Academy of Sciences, 5625 Renmin Street, Changchun 130022, People's Republic of China

Received April 9, 2006; Revised Manuscript Received August 4, 2006

ABSTRACT: We have followed the morphological evolution and crystallization process of spherical micelles formed by the mixture of polystyrene-*b*-poly(acrylic acid) (PS-*b*-PAA) and polystyrene-*b*-poly(2-vinylpyridine)-*b*-poly(ethylene oxide) (PS-*b*-P2VP-*b*-PEO) (the core of the spherical micelles was made of P2VP and PAA blocks through hydrogen bonding in neutral solvent *N*,*N*-dimethylformamide, DMF) via DMF vapor treatment. Different phenomena, such as rupture of the film, formation of cylinder aggregates and regular square lamellae, were observed when the micelle film was treated in DMF for different times. At the early stage of annealing in DMF vapor, the micelle film became unstable and ruptured. Cylinder aggregates, within which the PEO blocks achieved the association and primary chain folding, formed as the mesophases before the nucleation of the PEO single crystals at this stage. Further treatment in DMF vapor resulted in the nucleation of the PEO blocks at the corners of quasi-square lamellae. Then a quite regular "sandwich" lamellar structure, constructed by a PEO single-crystal layer covered by two tethered layers of other amorphous blocks on the top and bottom crystal basal surfaces, formed when the film of micelles was annealed in DMF vapor for sufficient times. It is found that the unique distribution of the crystallizable blocks in the film and the phase separation between the PS and PEO blocks in the corona of the initial micelles play an important role in the solvent-induced crystallization.

1. Introduction

The possible technological application of block copolymer thin films has been widely recognized, and various microphase separation structures have been observed in the experiments.[1,2] Each of these structures is generally nanoscale in size, ranging from 5 to 100 nm, and varies its morphology with slight changes of chemical structure and composition. In the copolymers made of noncrystalline segments, the repulsive force between the immiscible blocks is the main driving force in the phase separation. However, when one or more crystallizable segments are involved, the segment crystallization coupled with microphase separation will result in different ordered microstructures.[3] Microdomain geometry, strength of interblock repulsion, and the glass transition temperature of the amorphous blocks (T_g^a) have been considered as the major parameters that control the extent of confinement to the crystallization process.[4] A precise control of those factors will allow us to create higher-order and hierarchical structures.

Macromolecular self-organization process from core−shell nanoparticles on substrate has been investigated by Kimura group.[5] In the core of the particles on the substrate, the poly(L-lactide) (PLLA) blocks were partially crystallized. These particles collapse above the glass transition temperature of PLLA and the melting point of poly(ethylene oxide) to reaggregate into the parallel band structures, which are composed of PLLA crystal whose *c* axis is perpendicular to the substrate surface, while the *a* and *b* axes are perpendicular and parallel to the longitudinal direction of the bands, respectively. Liu et al. have explored the crystallization behavior within micellar core in dilute solid solutions and found that the stiffness of the amorphous block has considerable effect on the structure and morphology of the crystalline of the other blocks.[6] Wolff and co-workers have studied the effect of different surface potentials on the crystallization of spherical micelles at flat solid interfaces.[7] Xu and co-workers have also investigated the mechanism of crystallization and coalescence of block copolymer micelles with crystallizable cores in solution or melt,[8] and the results indicate that the length of each blocks mainly determine the crystalline and phase separation behaviors during the thermal treatment.

Many groups have proposed solvent vapor annealing because the temperature window, for developing ordered microphase separation structures, between glass transition and decomposition, is often insufficient for thermal equilibration.[2,9−12] In fact, the temperature window for inducing the crystallization of the crystallizable blocks is also inadequate for a great number of semicrystalline copolymers, considering the different thermal properties of each block. We may reduce the T_g^a lower than the T_c through solvent vapor treatment to obtain the softly confined crystallization of the crystallizable blocks, where the system will undergo hard confined crystallization during the thermal equilibrium. Solvent-induced crystallization has been investigated in detail on several important homopolymers and copolymers, such as poly(ethylene terephthalate), poly(ether ether ketone), polycarbonate, syndiotactic polystyrene, and ethylene−vinyl acetate.[13−15] It is a complex phenomenon involving the coupled processes of diffusion, swelling, and crystallization. In some sense, solvent-induced crystallization is a kind of "cold crystallization" by annealing from the glassy state because the sample does not undergo the melt state before crystallization. This should result in much difference from the common melt crystallization process. More significantly, the slow process of solvent-induced crystallization allows us to investigate the induction state before the nucleation and the subsequent growth of crystallization.[16−20] This is important for the theory analysis of the crystallization process since it is difficult to perform in melt crystallization.[21]

Herein we prepare block copolymer spherical micelles from blends polystyrene-*b*-poly(acrylic acid) (PS-*b*-PAA) diblock and

* Corresponding author: Tel 86-431-5262175; Fax 86-431-5262126; e-mail ychan@ciac.jl.cn.

10.1021/ma060799k CCC: $33.50
Published on Web 10/20/2006

polystyrene-*b*-poly(2-vinylpyridine)-*b*-poly(ethylene oxide) (PS-*b*-P2VP-*b*-PEO) triblock copolymers. Solvent vapor treatment induced the crystallization of spherical micelles with the formation of regular square lamella of PEO block as middle layer between the amorphous blocks. Because of the unique distribution of the crystallizable blocks in the system and the special constraint exerted by other blocks, the solvent-induced crystallization of micelles has a quite different morphological transition from the traditional crystallization of block copolymers from the melt state, especially for the induction period and the nucleation of the crystallization. The plausible thermodynamic analysis of the formation of square lamella has been investigated. Although solvent-induced crystallization has been successfully used to obtain perpendicular chain axis orientation on amorphous unoriented polymeric films,[22] the formation of more regular square lamellae of PEO blocks simply by solvent vapor treatment in our work is remarkable.

2. Experimental Section

2.1. Sample Preparation. Polystyrene-*b*-poly(acrylic acid) (PS-*b*-PAA) and polystyrene-*b*-poly(2-vinylpyridine)-*b*-poly(ethylene oxide) (PS-*b*-P2VP-*b*-PEO) were supplied by Polymer Source, Inc., and used as received. The number-averaged molecular weights of each block in the diblock and triblock copolymers are 16500 (PS), 4500 (PAA), 14100 (PS), 12300 (P2VP), and 35000 (PEO). Micelles were prepared by mixing 0.0068 g of PS-*b*-P2VP-*b*-PEO and 0.0064 g of PS-*b*-PAA in 6.6001 g of *N*,*N*-dimethylformamide (DMF) (purchased from Beijing Chemical Plant and used as received). The 2VP/AA molar ratio is about 0.7 to obtain uniform spherical micelles, and this parameter did not vary in our experiments. The solution was stirred for several days by a magnetic stir and then stored at room temperature for 3 months to achieve equilibrium state. All samples in this paper were prepared from the same solution, with the total weight concentration of 0.2%. The silicon wafers were cleaned in a piranha solution (70/30 v/v of concentrated H_2SO_4 and 30% H_2O_2, *hazardous* solution!) at 90 °C for 20 min, thoroughly rinsed with deionized water, and finally blown dry with nitrogen. Micelle samples for TEM were prepared by dipping a droplet of the micellar solution on a carbon-coated copper grid. The excess solution was blotted away with filter paper, and the remaining solvent was slowly evaporated in air at room temperature. Uniform thin films were prepared by spin-coating the micelle solution onto the precleaned silicon wafer or freshly cleaved mica using a commercial spin-coater KW-4A, Chemat Technology Inc. The spin-coating speed was kept at 2500 rpm for all samples.

2.2. Sample Treatment. The films were subsequently put in a closed desiccator with sufficient liquid DMF for certain period at room temperature. Two kinds of approaches have been introduced to track the dynamic process of the solvent-induced crystallization. The first approach is to treat a group of samples prepared under the same condition for different periods. The second approach is to treat one sample for several times. That is, after the solvent vapor treatment and the subsequent characterization, the same sample was then exposed to the vapor for a second treatment. During the second period, further crystalline would develop in the film.[14] After each vapor treatment, the films were dried in a vacuum oven at room temperature for a long time to remove the remaining solvent molecules within the samples. The experimental results prove that the two approaches have similar effect on the solvent-induced crystallization.

The films after treated with DMF vapor were floated onto a water bath and then transferred to the copper grids and dried in a vacuum for transmission electron microscopy (TEM) characterization.

2.3. Characterization. To confirm the hydrogen bonding between the P2VP and PAA blocks, Fourier transform infrared (FTIR) spectra were taken with a Bruker evacuable IFS 66v/S (liquid nitrogen cooled MCT detector). The spectra were collected at a resolution of 4 cm^{-1}, and 512 scans were coadded to achieve the desired signal-to-noise ratio. Samples were prepared on the silicon wafer and kept under vacuum (≈5 mTorr) during acquiring spectra data.

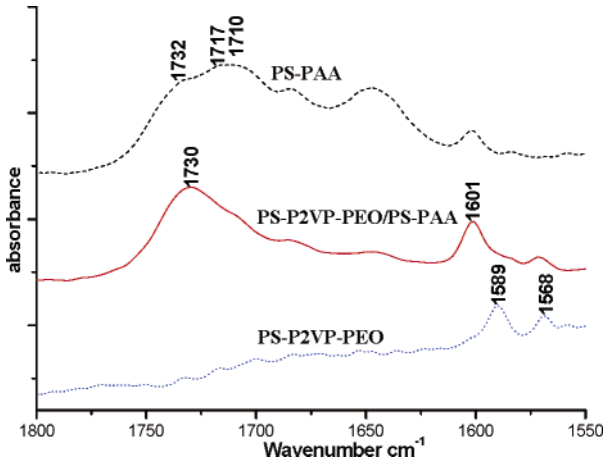

Figure 1. FTIR spectra of (black dash) PS-*b*-P2VP-*b*-PEO, (blue dot) PS-*b*-PAA, and (red solid) PS-*b*-P2VP-*b*-PEO/PS-*b*-PAA micelles dipped onto the Si wafer.

The morphologies of the micelles were investigated by TEM and atomic force microscopy (AFM). TEM experiments were carried out in a JEOL (JEM-1011) TEM using an accelerating voltage of 100 kV. Micelle samples for TEM were prepared by dipping a droplet of the micellar solution on a carbon-coated copper grid. The sample-loaded grid was observed directly without staining. AFM images were acquired on a commercial SPA300HV/SPI3800N Probe Station, Seiko Instruments Inc., Japan, in tapping mode. A silicon microcantilever (spring constant 2 N/m and resonance frequency ~70 kHz, Olympus Co., Japan) with an etched conical tip (radius of curvature ~40 nm as characterized by scanning over very sharp needle array, NT-MDT, Russia) was used for scan. AFM characterization was performed on those thin films on mica before and after the solvent vapor treatment. The X-ray photoelectron spectroscopy (XPS) was measured with VG ESCALAB MK II at room temperature by using an Al Kα monochrom ($h\nu = 1486.6$ eV) at 14 kV and 20 mA. The sample analysis chamber of the XPS instrument was maintained at a pressure of 8×10^{-8} Pa. The contact angles of films were estimated by DSA10-MK2 (Krüss GmbH, Germany) at the ambient temperature. Water droplets (about 5 mg) were dropped carefully onto the films.

3. Results and Discussion

In this section, we start by characterization the spherical micelles prepared by the mixture of polystyrene-*b*-poly(acrylic acid) (PS-*b*-PAA) and polystyrene-*b*-poly(2-vinylpyridine)-*b*-poly(ethylene oxide) (PS-*b*-P2VP-*b*-PEO) in neutral solvent *N*,*N*-dimethylformamide (DMF). We then show the morphological evolution and crystallization process of the spherical micelle film during the DMF vapor treatment. Finally, we give the plausible mechanism for the morphological transition and the formation of regular lamellae based on the unique distribution of the crystallizable blocks in the film and the phase separation between the PS and PEO blocks.

3.1. Formation of Spherical Micelles in DMF. Hydrogen bonding should occur between vinylpyridine and carboxylic acid as observed elsewhere.[23] Although hydrogen bonding between the PAA and PEO blocks cannot be neglected, it should be much weaker than that between P2VP and PAA.[23,24] Fourier transform infrared (FTIR) was used to prove the existence of hydrogen bonding between the P2VP and PAA blocks (Figure 1). In the carbonyl region, for the spectrum of PS-*b*-PAA (Figure 1, black dashed line), the bands near 1732 and 1710 cm^{-1} correspond to the free carboxyl group and the dimer of acrylic acid units,

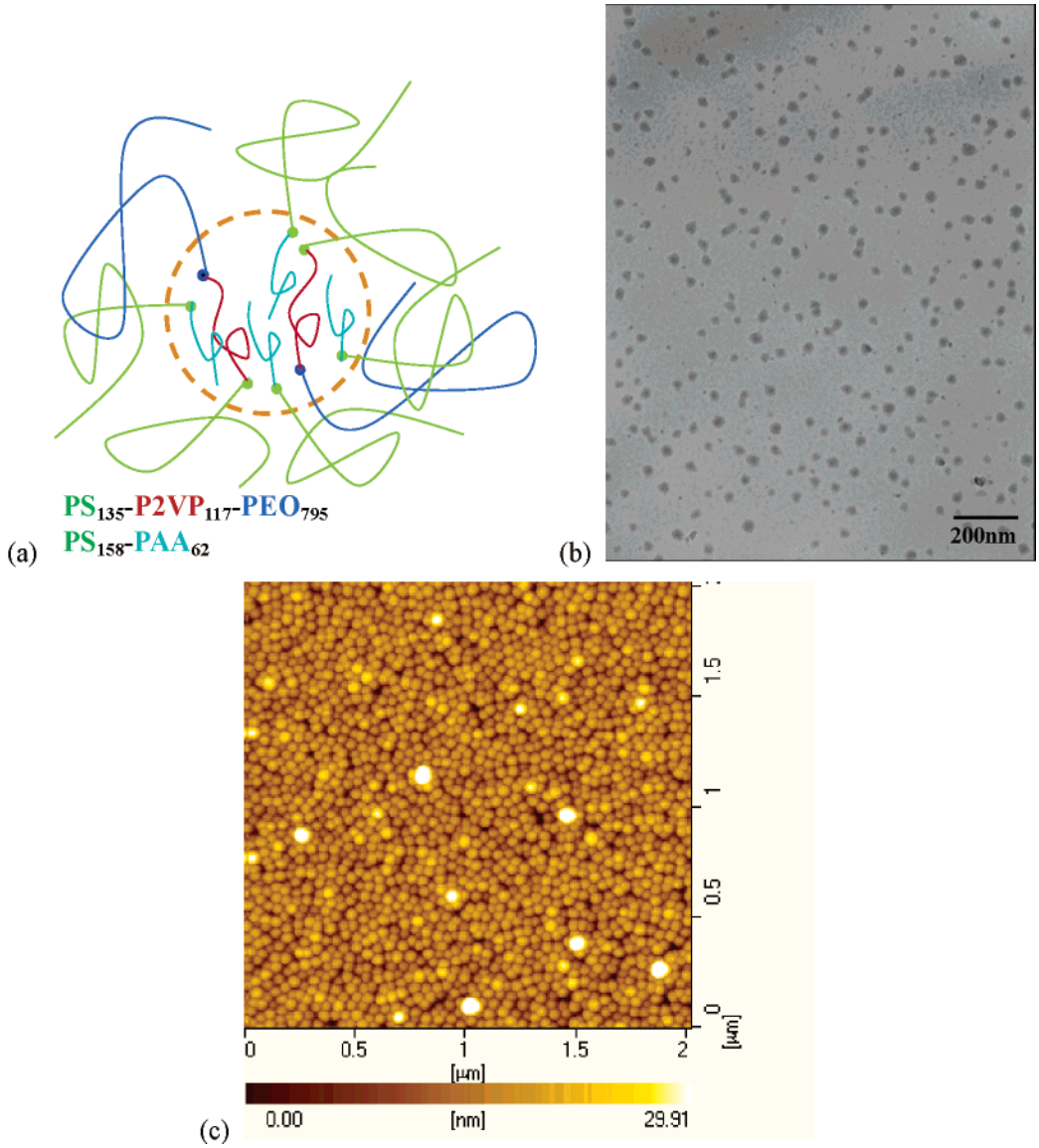

Figure 2. (a) A model representation, (b) TEM micrograph, and (c) AFM height image of PS-*b*-P2VP-*b*-PEO/PS-*b*-PAA micelles.

respectively.[25,26] While in the spectrum of the blend (Figure 1, red solid line), the C═O stretching vibration appeared at 1730 cm^{-1}, indicating the carboxyl groups were in a less associated state than that in pure PS-*b*-PAA. Moreover, in the pyridine region, for the spectrum of PS-*b*-P2VP-*b*-PEO (Figure 1, blue dotted line), the absorption of pyridine group is located at 1589 and 1568 cm^{-1}. The phenyl group of the styrene units in PS-*b*-PAA and PS-*b*-P2VP-*b*-PEO exhibit a strong and a very weak absorption at 1601 cm^{-1}, respectively. In the blend spectrum (Figure 1, red solid line), the band intensity of 1589 cm^{-1} is greatly decreased. Compared with the spectra of PS-*b*-PAA and PS-*b*-P2VP-*b*-PEO, the band intensity increase at 1601 cm^{-1} is an overlap of the phenyl groups and the complex pyridine groups, which results from a perturbation of the 1589 cm^{-1} ring mode.[25] These results indicate the formation of complex between carboxyl group and pyridine nitrogen in the solution.

DMF is a good solvent for both PS and PEO blocks, thus leading to micelles with a P2VP/PAA core surrounded by a mixed corona of PS and PEO blocks in DMF solution of PS-*b*-PAA and PS-*b*-P2VP-*b*-PEO blends (Figure 2a). Parts b and c of Figure 2 show the representative TEM and AFM images of micelles, respectively. We can also observe some cylinders; however, spherical micelle was the dominate morphology.

3.2. Solvent-Induced Crystallization of Spherical Micelles. AFM characterization was performed on a series of samples of Figure 2c treated with DMF vapor for different times (Figure 3). The film prepared by spin-coating the micelle solution on mica was made up of two or three layers of compact packing micelles, as shown in Figure 2c. However, the flat film of micelles became unstable and would rupture in the DMF vapor.[27] After 2 h exposure to saturated DMF vapor, there were numerous holes, gaps (Figure 3a), and terraces (Figure 3a′, image has been flattened for clarity) on the top of an absorbed layer on the substrate. Many cylinders parallel with the horizontal formed within the terraces. The diameter of these cylindrical aggregates was similar to that of the original spherical micelles. Detailed structure of these cylindrical aggregates will be discussed in next section. Further solvent vapor treatment (10 h) induced the formation of islands with quasi-square shape (Figure 3b). These islands were the result of the further shrinkage of the ruptured film. Each of them had a rim around the flat central areas. Eventually (50 h), regular square lamellae with the thickness of about 32 nm (Figure 3c) formed. From the profile of the cross section in Figure 3c, some of these lamellae had another small lamella with same height upon them, which was familiar in the crystallization of polymers. The

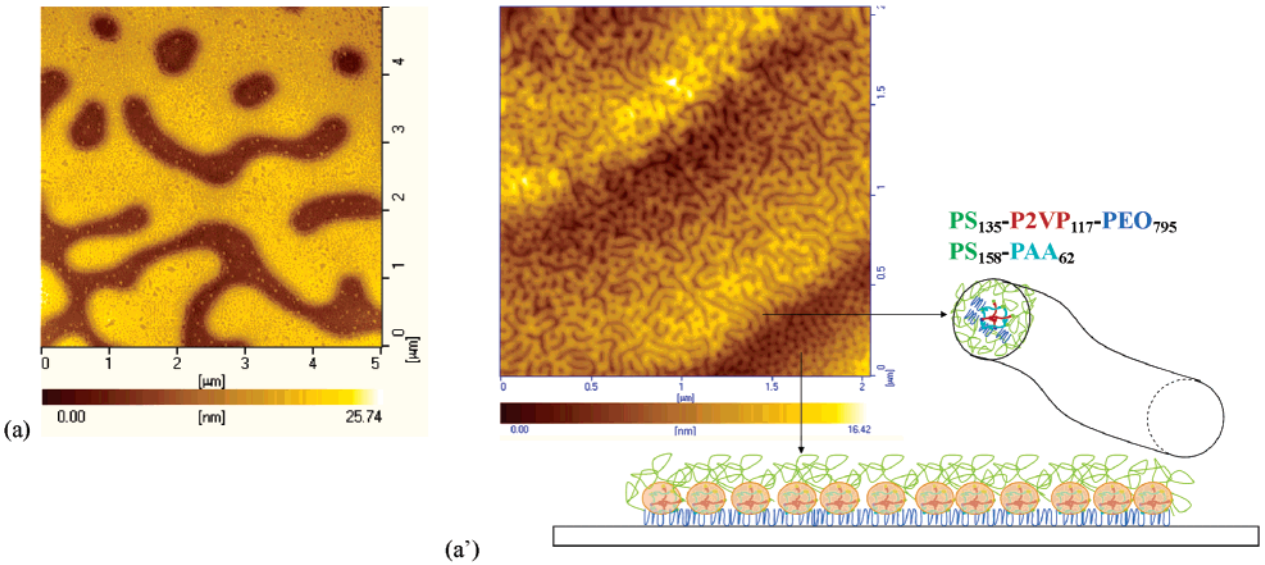

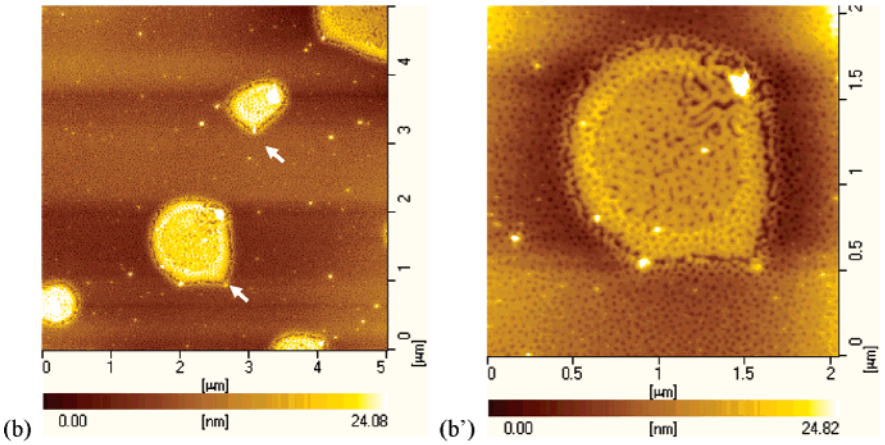

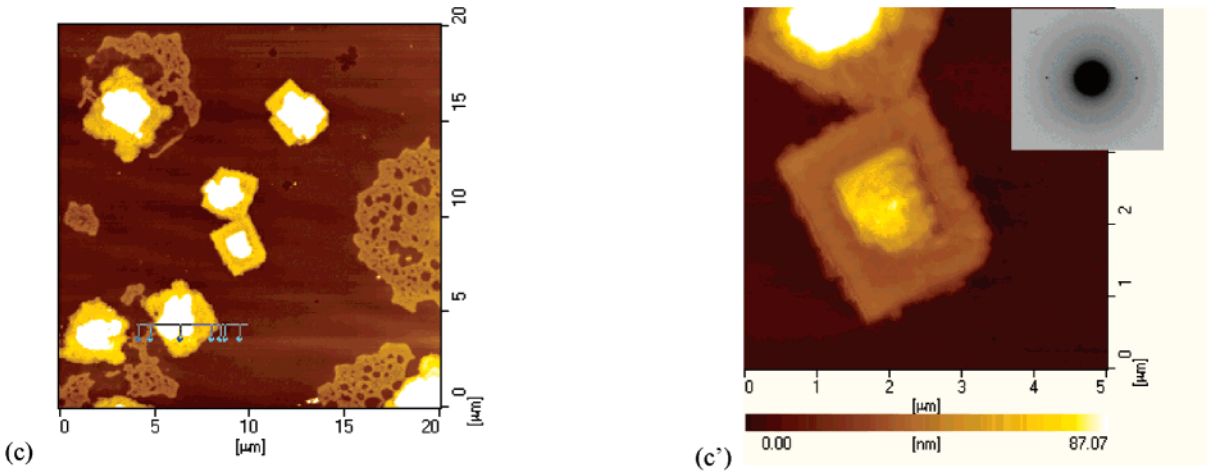

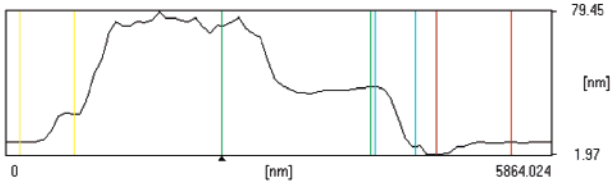

	Z1[nm]	Z2[nm]	ΔZ [nm]	Distance [nm]	Φ[°]
	2.281865	9.388836	7.106972	803.2910	0.506901
	9.54027	24.83499	15.29472	585.2549	1.496995
	39.33965	7.141644	32.19800	436.0722	4.222851
	72.13538	39.25074	32.88463	1606.582	1.172606

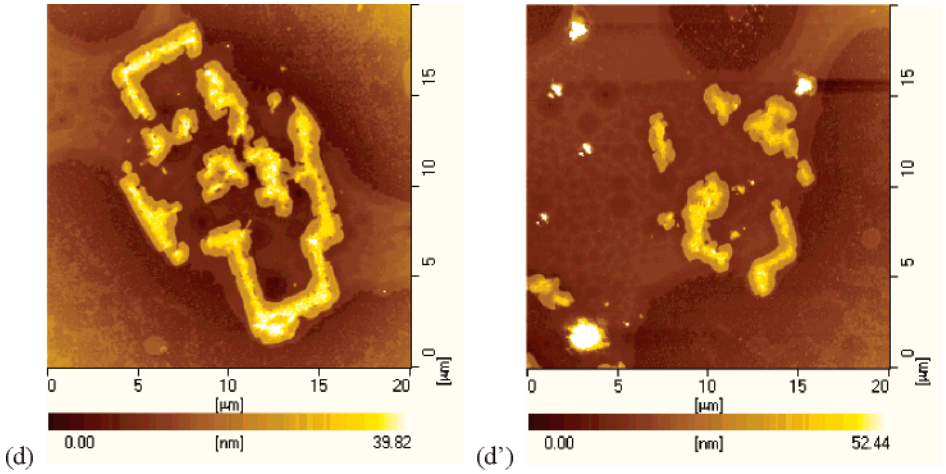

Figure 3. AFM height images of the sample of Figure 2 after exposed to DMF vapor for different times: (a, a′) 2 h, (b, b′) 10 h, (c, c′) 50 h, (d, d′) 204 h. Inset of (c′) is the electron diffraction of the square crystalline. The right plot of (c) is its profile of cross-section analysis.

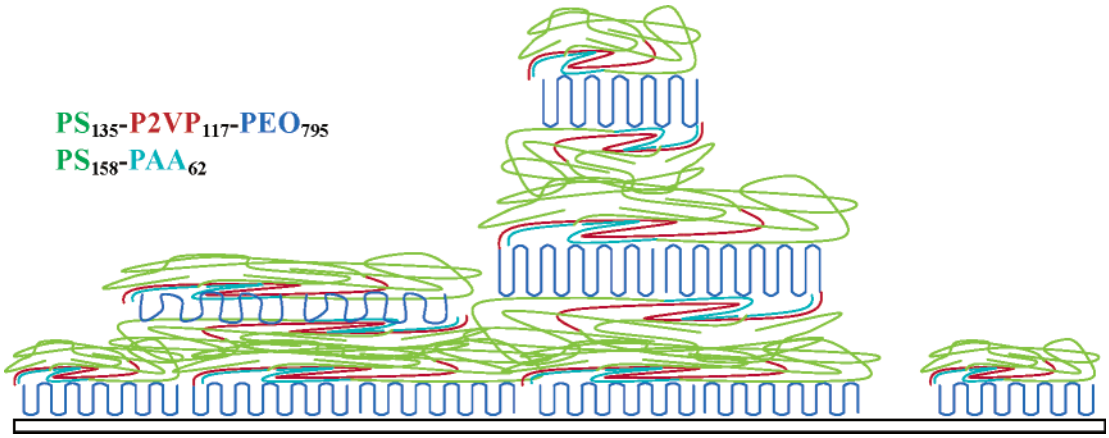

Figure 4. Schematics of the structure of multilayer lamellae of PEO single crystals.

regular shape of square lamella was similar to that of the single crystal of PS-*b*-PEO from dilute solution.[28,29] This can be further proved by the pair of electron diffraction spots, which are attributed to the two (120) planes (inset of Figure 3c′). The absence of another pair of diffraction spots may be caused by the oblique structure,[30] or the highly beam sensitivity of the crystalline, or the destruction in the water during the sample preparation. From the shape and the thickness we presume that the possible structure of our lamella is also the "sandwich" structure with chain folding of PEO covered with two layers of amorphous blocks (Figure 4). When the film was annealed in the vapor for even longer times (up to 204 h), these square lamellae decomposed into dropletlike crystalline patches (Figure 3d).

The change of the composition of the surface of the film during the solvent annealing is confirmed by both XPS experiments and water contact angle measurements. Figure 5 shows the XPS C 1s spectra with fitted peaks for the film before (Figure 5a) and after (Figure 5b) the solvent vapor treatment for 50 h. The envelope can be resolved into two chemical components: C−C/C−H at 284.6 eV and ethoxy group carbon in PEO at 286.1 eV.[31] The relative intensity of the C−O peak decreased after the solvent vapor treatment, which implies the reduction of the PEO fraction in the surface of the film. Because PS−PAA was excessive, with respect to PS−P2VP−PEO (2VP/AA molar ratio was 0.7), some uncomplexed PS−PAA molecules (did not form hydrogen bonding with PS−P2VP−PEO) would be randomly deposited on the substrate during the spin-coating. So the PAA signals (peak at 289 eV) are observed on the sample before solvent vapor treatment. But this peak greatly decreased after the film was annealed in DMF vapor for 50 h. During annealed in DMF vapor, PS blocks of the uncomplexed PS−PAA molecules would move to the surface of the film because of the lower surface energy ($\gamma_{PS} \approx 40$ mN/m,[32] $\gamma_{PAA} \approx 60$ mN/m[33]). On the other hand, the N 1s peak in the XPS spectrum was quite weak because most PS−P2VP−PEO formed hydrogen bonding with PS−PAA.

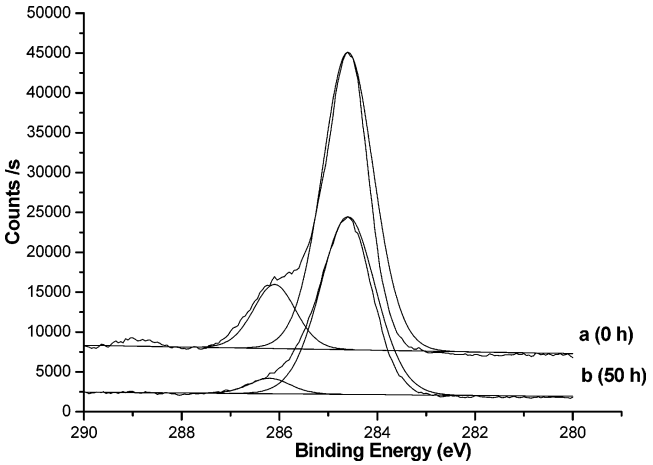

Figure 5. High-resolution C 1s spectra with fitted curves for the samples of (a) Figure 2c and (b) Figure 3c.

The initial film composed of spherical micelles had a contact angle against water of about 30°, and the water droplet was absorbed in several seconds, which shows that the surface must be partially covered with hydrophilic blocks. However, the film after treated in DMF vapor for 2 h or longer times had a contact angle against water of about 90°, which shows that the surface must be mainly covered with hydrophobic PS blocks. Although the surface of thin films before and after annealed in DMF vapor were both rough, the surface roughness did not play a significant role as the effect of surface roughness was to amplify the wetting. If the surface was mainly covered by hydrophilic materials, such as PEO, PAA, and P2VP blocks, the roughness would increase the hydrophilicity and then decrease the contact angle against water.[34] As the films annealed in DMF vapor for certain period had the contact angles against water of about 90°, the surface should be mainly covered by PS blocks, the sole hydrophobic part in the blend system.

XPS and contact angle experiments indicate that the surface chemistry of the film changes from mixture of PS and PEO to almost all PS after treated in DMF vapor for certain period.

3.3. Mechanism of Morphological Evolution. From above experimental results, the solvent-induced crystallization of the spherical micelles of PS-*b*-PAA/PS-*b*-P2VP-*b*-PEO can be divided into three different stages, namely, rupture of the flat film, nucleation of PEO blocks at the thicker areas of the film, and formation of regular square lamellae. During these stages, local chain ordering into small clusters, coalescing of the clusters into small lamellae, and completion of a single lamella will occur, respectively, as revealed by molecular dynamics simulation of polymer crystallization through chain folding.[35] Two factors are crucial for the formation of the regular square lamellae: the unique distribution of the crystallizable blocks in the film and the phase separation between the PS and PEO blocks.

Different from the common therm-induced crystallization which is started from random melt, the structure of the spherical micelles renders a special distribution of the crystallizable blocks in the film, since all PEO blocks are located in the corona of the spherical micelles. This distribution resembles neither the complete random states in the melt nor the regular pattern in the phase separated film, and few detailed studies have been concerned with this kind of system. We will show that the unique distribution of the crystallizable PEO blocks in the film has essential influence on the morphological evolution of the film at the above-mentioned three stages during the solvent treatment.

The first stage of the solvent-induced crystallization of micelles is the rupture process. Because of the rapid evaporation of the solvent during the spin-coating, the micelles in the solution were randomly deposited on the substrate. Although the spherical micelles are thermodynamic equilibrium state in DMF solution, annealing in DMF vapor will lead to the rupture of the film (Figure 3a). This rupture process of the film is quite similar to the autophobic dewetting process in diblock copolymer and homopolymer films.[36] The drive force of the rupture is the difference in entropy between the absorbed and free polymers resulting from the different chain conformations.[21] Each polymer segment in contact with the substrate gains certain adsorption energy, and therefore the molecules are attracted to the substrate. It is found that the PEO blocks are more compatible to a SiO_x layer or mica surface than the nonpolar hydrogenated poly(butadiene)[37] and PS.[38] Thus, the PEO blocks are expected to form an adsorbed layer on mica, as shown at the bottom of Figure 3a′. Above this absorbed layer of PEO on the substrate, we can observe many cylinders parallel with the horizontal within the terraces (Figure 3a′).

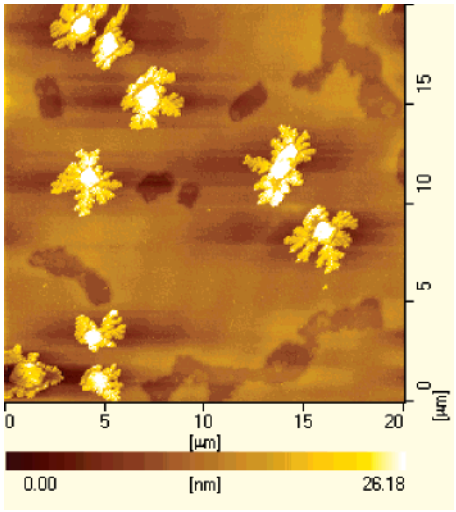

Figure 6. AFM height image of the film made up of micelles of PS-*b*-P2VP-*b*-PEO after exposed to DMF vapor for 69 h.

In fact, these cylinders can be regarded as the evidence of the phase separation between the PS and PEO in the corona of the spherical micelles during the solvent treatment. When the spherical micelles are treated in DMF vapor, the aggregation and primary folding of the PEO blocks in the corona of the micelles will result in the unfavorable contact between the solvent molecules and the PEO blocks because the solvent molecules are difficult to enter the compactly folded chains in the solvent-induced crystallization.[13] Then the total number of chains in the corona of the micelle will reduce and the volume of the core will expand, which simultaneously increase the deformation energy of the micelle. In this case, a sphere-to-rod morphological transition is expected to occur to decrease the entropy penalty.[39,40] The PEO blocks and the insoluble micellar core, P2VP and PAA blocks linked by hydrogen bonding, are surrounded by the swollen PS blocks in the DMF vapor as shown on the right of Figure 3a′.

Besides the unique distribution of the crystallizable blocks in the film rendered by the spherical structure of the micelles, the other crucial factor determining the morphological evolution of the film during the solvent treatment is the phase separation of the PS and PEO blocks in the corona of the spherical micelles. For comparison, we also prepare spherical core−shell−corona micelles from pure PS-*b*-P2VP-*b*-PEO in water.[41] In this case, the corona of the micelle consists of PEO blocks. When the film composed of this kind of micelles is annealed in the DMF vapor, only irregular dendritic lamellae form (Figure 6). Without the phase separation between the PS and PEO blocks, PEO blocks in the corona of these micelles can easily coalesce and nucleate during the solvent treatment which results in the formation of less regular crystals (Figure 6). Thus, the phase separation between the PS and PEO blocks in the corona of spherical micelle from mixture of PS-*b*-PAA and PS-*b*-P2VP-*b*-PEO is responsible for the formation of regular square lamellae during the solvent-induced crystallization. Actually, the local chemical and physical environments provided for polymer crystallization can enhance polymer crystallization, such as crystallization from a preordered state rather than in the isotropic state, or hamper it, such as crystallization under "self-poisoning" or in amorphous−crystalline polymer blends or under different nonoconfinements.[28]

Now we will discuss the occurrence of the phase separation between the PS and PEO blocks in the corona of the spherical micelles based on dilution approximation theory. Phase separation is a familiar phenomenon during the solvent vapor treatment of block copolymers.[9] For a given copolymer composition *f*, if the solvent is neutral or good, the mean-field order−order transitions (OOT) and order−disorder transitions (ODT) can be obtained from the melt phase map by replacing $\chi_{AB}N$ with $\varphi\chi_{AB}N$ in the concentrated regime and $\varphi^{1.59}\chi_{AB}N$ in the semidilute regime, with χ_{AB}, N, and φ denoting the Flory−Huggins interaction parameter between A and B, the total degree of polymerization, and the copolymer concentration, respectively.[42−44] For dilute solution of neutral solvents, the effective A/B interaction parameter (χ_{eff}) should be much lower.[45] Then PS and PEO blocks mixed in the corona of the spherical micelles. It is found that the ordering of the PS-*b*-PEO copolymer film swollen with benzene vapor is lost when the copolymer volume fraction is less than ~0.9.[9] This result is consistent with the dilute approximation theoretical calculation as follow. Because the PS weight fraction of this copolymer is 0.75, the $(\chi N)_{ODT}$ is about 18.[46] On the other hand, the χN of this copolymer in the bulk at room temperature is about 20.9, since the mean-field segmental interaction parameter between the styrene and ethylene oxide is $\chi(T) = -0.00705 + 21.3/T$.[47] Thus, we can get the critical copolymer volume concentration of order−disorder transition, 0.86 or 0.91, based on the above-mentioned model of concentrated or semidilute solution, respectively. When the copolymer volume fraction is high than ~0.9, the strength phase separation (χN) of this system is larger than the $(\chi N)_{ODT}$. Then the phase separation between PS and PEO blocks will begin from the surface and propagate through the film which causes the development of highly ordered arrays of nanoscopic cylindrical domains with high aspect ratios over long-range lateral order.[9]

In our experiments, the vapor pressure of DMF at room temperature (4.0 mmHg) is much lower than that of benzene (95.8 mmHg).[48] So the saturated polymer concentration in our system must be much higher than that of PS-*b*-PEO film in benzene vapor (0.69).[9] The degree of segregation ($\chi_{AB}N$) between the PS and PEO blocks in bulk state at room temperature is about 59.9 ($\chi = 0.0644$, $N_{PS} = 135$, $N_{PEO} = 795$).[47] Then the χN in the DMF swollen film is expected to be greatly larger than 33.2 ($0.69 \times 59.9 = 41.3$, $0.69^{1.59} \times 59.9 = 33.2$, based on above-mentioned model of concentrated or semidilute solution). Phase separation between the PS and PEO blocks in the corona of the micelles should occur during the solvent treatment[49,50] as long as these blocks have sufficient mobility. When the micelles formed in the dilute DMF solution, the PS and PEO blocks are intermingled because of the shield effect of the neutral solvent. Thus, the phase separation between the PS and PEO blocks in the corona of the micelles is crucial for the nucleation and subsequent growth of the crystallization of PEO blocks in the early stage.[51] The phase separation in the corona of the micelles also promotes the formation of "sandwich" structure in the swollen film, and similar effects on the self-assembly in bulk or solution have been discussed concerning the morphology of micelles or vesicles.[23,49,52−55] A detailed discussion about the dynamic coupling and competition between microphase separation and crystallization of PS-*b*-PEO can be found in ref 51.

In the first stage "empty surface" were created as the area occupied by an amorphous PEO blocks is large than the area needed by a crystallized blocks. As a consequence, a depletion zone was created just ahead of the crystal (Figure 3a). At the same time, terraces were simultaneously formed at certain place during the rupture of the film. The cylinders form as mesophases during the induction period of crystallization.[16−20] The formation of these cylinders will facilitate the further crystallization of the PEO chains.[56] The irregular shapes of the holes and the gaps in Figure 3a can be understood since the PEO blocks in the corona of the micelles were randomly distributed in the film. These holes, gaps, and terraces in the film would develop and evolve to islands of quasi-square shape in the process of further solvent annealing (Figure 3b), which brings the solvent-induced crystallization to the second stage.

During the second stage, the PEO blocks are highly condensed between the amorphous blocks. From the quasi-square shape we presume that nucleation for the PEO single crystal already happens at the corners of these isolated islands (indicated by the white arrows in Figure 3b), and the PEO chains achieve more regular fold in the cylinders and the stems direction is almost normal to the substrate. It has been pointed out that the cylinders developed by the microphase separation in the melt generally guide the growth of the crystallization but do not completely confine them and a large volume of material can be crystallized together from a single nucleus.[56,57] In the case of spherical micelles, PEO blocks were randomly distributed in the corona of each micelle. The thin film underwent slow morphological transformation due to the incontinuous crystallizable blocks. When cylinder aggregates formed, PEO blocks could easily achieve aggregation and subsequent folding, which could promote the crystallization rate.

At the final stage, regular folding of PEO chains is achieved after sufficient time of solvent annealing (Figure 3c). From the height image and profile of cross section in Figure 3c, we present a model of the multilayered lamellae in Figure 4. It should be noted that we do not draw the small quantity of free PS−P2VP−PEO and PS−PAA molecules which did not form hydrogen bonding in the solution and the thin film. Because of the strong interaction between the PEO blocks and the mica, those micelles contacted with the substrate in the initial film were fixed on the substrate and thus cannot form long stem (total thickness of the adsorbed layer is about 7 nm) as those lamellae on the top of them (total thickness of the sandwich structure is about 32 nm) during the solvent-induced crystallization. Besides the regular lamellae, there are another layer with large areas and lower regularity on the adsorbed layer. The thickness (~15 nm) is about half of the thickness of the square lamellae (~32 nm) and twice of the thickness of the adsorbed layer (~7 nm). So this layer also possesses sandwich structure and PEO blocks in the middle layer achieve less ordered folding, with respect to the square lamellae (Figure 4), corresponding to a more ordered and stable thermodynamic equilibrium state.[38]

However, the folded chain crystals are not in thermodynamic equilibrium, with respect to the fully extended chain crystals. Reorganization within polymer lamellae will happen when the sample is annealed for longer times or at temperatures near the melting point.[21,38] Since chains at the edge of the crystal are much mobile compared to the interior, chain relaxations within the lamellae start there, and a pronounced rim is formed around those square lamellae after stored in air at room temperature for several months (images not shown). If the film of spherical micelles was treated in the DMF vapor for long times (up to 204 h), dropletlike crystalline patches locating at the boundary of the imaginary square lamellae can be observed on the substrate (Figure 3d). These excessively annealed films are very similar to the results of Reiter.[38]

4. Conclusion

The morphological transition and crystallization process of the spherical micelles of PS-*b*-PAA/PS-*b*-P2VP-*b*-PEO with the core made of P2VP and PAA blocks have been investigated in DMF vapor treatment. At the early stage of annealing in the DMF vapor, the film become unstable and ruptures. Cylinder aggregates, within which the PEO blocks achieve the association and primary chain folding, form as the mesophases before the nucleation of the PEO single crystals at this stage. Further treatment in DMF vapor results in the nucleation of the PEO blocks. Then a quite regular "sandwich" lamellar structure, constructed by a PEO single-crystal layer covered by two tethered layers of other amorphous blocks on the top and bottom crystal basal surfaces, forms when the film of micelles is annealed in DMF vapor for sufficient time. It is found that the unique distribution of the crystallizable blocks in the film and the phase separation between the PS and PEO blocks in corona of the initial micelles play an important role in the solvent-induced crystallization.

Acknowledgment. This work was subsidized by the National Natural Science Foundation of China (20334010, 20474065, 50573077).

References and Notes

(1) Fasolka, M. J.; Mayes, A. M. *Annu. Rev. Mater. Res.* **2001**, *31*, 323.
(2) Segalman, R. A. *Mater. Sci. Eng. R* **2005**, *48*, 191.
(3) Fu, J.; Luan, B.; Yu, X.; Cong, Y.; Li, J.; Pan, C.; Han, Y.; Yang, Y.; Li, B. *Macromolecules* **2004**, *37*, 976.
(4) Huang, Y.-Y.; Yang, C. H.; Chen, H.-L.; Chiu, F.-C.; Lin, T.-L.; Liou, W. *Macromolecules* **2004**, *37*, 486.
(5) (a) Fujiwara, T.; Miyamoto, M.; Kimura, Y. *Macromolecules* **2000**, *33*, 2782. (b) Fujiwara, T.; Miyamoto, M.; Kimura, Y.; Sakurai, S. *Polymer* **2001**, *42*, 1515. (c) Fujiwara, T.; Miyamoto, M.; Kimura, Y.; Iwata, T.; Doi, Y. *Macromolecules* **2001**, *34*, 4043.
(6) Liu, L.-Z.; Jiang, B. *J. Polym. Sci., Part B* **1998**, *36*, 2961.
(7) Wolff, M.; Scholz, U.; Hock, R.; Magerl, A.; Leiner, V.; Zabel, H. *Phys. Rev. Lett.* **2004**, *92*, 255501.
(8) (a) Xu, J. T.; Jin, W.; Liang, G. D.; Fan, Z. Q. *Polymer* **2005**, *46*, 1709. (b) Xu, J. T.; Fairclough, J. P. A.; Mai, S. M.; Ryan, A. J. *J. Mater. Chem.* **2003**, *13*, 2740.
(9) Kim, S. H.; Misner, M. J.; Xu, T.; Kimura, M.; Russell, T. P. *Adv. Mater.* **2004**, *16*, 226.
(10) Fukunaga, K.; Hashimoto, T.; Elbs, H.; Krausch, G. *Macromolecules* **2002**, *35*, 4406.
(11) Xuan, Y.; Peng, J.; Cui, L.; Wang, H.; Li, B.; Han, Y. *Macromolecules* **2004**, *37*, 7301.
(12) Peng, J.; Xuan, Y.; Wang, H.; Yang, Y.; Li, B.; Han, Y. *J. Chem. Phys.* **2004**, *120*, 11163.
(13) McPeak, J. L. PhD Thesis, Virginia Polytechnic Institute and State University, 1999.
(14) Harron, H. R.; Pritchard, R. G.; Cope, B. C.; Goddard, D. T. *J. Polym. Sci., Part B* **1996**, *34*, 173.
(15) Shieh, Y.-T.; Lin, Y.-G. *J. Appl. Polym. Sci.* **2003**, *87*, 1144.
(16) Strobl, G. R. *Eur. Phys. J. E* **2000**, *3*, 165.
(17) Imai, M.; Kaji, K.; Kanaya, T. *Phys. Rev. Lett.* **1992**, *71*, 4162.
(18) Akpalu, Y. A.; Amis, E. J. *J. Chem. Phys.* **2000**, *113*, 392.
(19) Kawai, T.; Sakamoto, Y.; Kimura, T. *Mater. Trans., JIM* **2000**, *41*, 955.
(20) Kikkawa, Y.; Abe, H.; Iwata, T.; Inoue, Y.; Doi, Y. *Biomacromolecules* **2001**, *2*, 940.
(21) Sommer, J.-U., Reiter, G., Eds. *Lect. Notes Phys.* **2003**, *606*, 1.
(22) Rizzo, R.; Guardia, S. D.; Guerra, G. *Macromolecules* **2004**, *37*, 8043.
(23) Gohy, J.-F.; Khousakoun, E.; Willet, N.; Varshney, S. K.; Jérôme, R. *Macromol. Rapid Commun.* **2004**, *25*, 1536.
(24) Gohy, J.-F.; Varshney, S. K.; Jérôme, R. *Macromolecules* **2001**, *34*, 3361.
(25) Jiang, S.; Göpfert, A.; Abetz, V. *Macromolecules* **2003**, *36*, 6171.
(26) Hao, E.; Lian, T. *Chem. Mater.* **2000**, *12*, 3392.
(27) Reiter, G.; Sommer, J.-U. *Phys. Rev. Lett.* **1998**, *80*, 3771.
(28) Chen, W. Y.; Li, C. Y.; Zheng, J. X.; Huang, P.; Zhu, L.; Ge, Q.; Quirk, R. P.; Lotz, B.; Deng, L.; Wu, C.; Thomas, E. L.; Cheng, S. Z. D. *Macromolecules* **2004**, *37*, 5292.
(29) (a) Lotz, B.; Kovacs, A. J. *Kolloid Z. Z. Polym.* **1966**, *209*, 97. (b) Lotz, B.; Kovacs, A. J.; Bassett, G. A.; Keller, A. *Kolloid Z. Z. Polym.* **1966**, *209*, 115.
(30) Baltá Calleja, F. J.; Hay, I. L.; Keller, A. *Kolloid Z. Z. Polym.* **1966**, *209*, 128.
(31) Ton-That, C.; Shard, A. G.; Daley, R.; Bradley, R. H. *Macromolecules* **2000**, *33*, 8453.
(32) Wu, S. In *Polymer Handbook*, 4th ed.; Brandrup, J., Immergut, E. H., Grulke, E. A., Abe, A., Bloch, D. R., Eds.; John Wiley and Sons: New York, 1999; p 521.
(33) Gong, J. P.; Kii, A.; Xu, J.; Hattori, Y.; Osada, Y. *J. Phys. Chem. B* **2001**, *105*, 4572.
(34) (a) Bico, J.; Marzolin, C.; Quéré, D. *Europhys. Lett.* **1999**, *47*, 220. (b) Wenzel, R. N. *Ind. Eng. Chem.* **1936**, *28*, 988. (c) Wenzel, R. N. *J. Phys. Colloid Chem.* **1949**, *53*, 1466.
(35) Yamamoto, T. *J. Chem. Phys.* **1997**, *107*, 2653.
(36) Limary, R.; Green, P. F. *Macromolecules* **1999**, *32*, 8167.
(37) Opitz, R.; Lambreva, D. M.; de Jeu, W. H. *Macromolecules* **2002**, *35*, 6930.
(38) Reiter, G. *J. Polym. Sci., Part B* **2003**, *41*, 1869.
(39) Zhang, L.; Eisenberg, A. *Macromolecules* **1999**, *32*, 2239.
(40) Lei, L.; Gohy, J.-F.; Willet, N.; Zhang, J.-X.; Varshney, S.; Jérôme, R. *Macromolecules* **2004**, *37*, 1089.
(41) Gohy, J.-F.; Willet, N.; Varshney, S.; Zhang, J.-X.; Jérôme, R. *Angew. Chem., Int. Ed.* **2001**, *40*, 3214.
(42) Huang, H.; Hu, Z.; Chen, Y.; Zhang, F.; Gong, Y.; He, T.; Wu, C. *Macromolecules* **2004**, *37*, 6523.
(43) de la Cruz, M. O. *J. Chem. Phys.* **1989**, *90*, 1995.
(44) Fredrickson, G. H.; Leibler, L. *Macromolecules* **1989**, *22*, 1238.
(45) Helfand, E.; Tagami, Y. *J. Chem. Phys.* **1972**, *56*, 3592.
(46) Leibler, L. *Macromolecules* **1980**, *13*, 1602.
(47) Zhu, L.; Cheng, S. Z. D.; Calhoun, B. H.; Ge, Q.; Quirk, R. P.; Thomas, E. L.; Hsiao, B. S.; Yeh, F.; Lotz, B. *Polymer* **2001**, *42*, 5829.
(48) *Chemical Properties Handbook*; Yaws, C. L., Ed.; McGraw-Hill: New York, 1999.
(49) Schrage, S.; Sigel, R.; Schlaad, H. *Macromolecules* **2003**, *36*, 1417.
(50) Hui, T.; Chen, D.; Jiang, M. *Macromolecules* **2005**, *38*, 5824.
(51) Li, L.; Séréro, Y.; Koch, M. H. J.; de Jeu, W. H. *Macromolecules* **2003**, *36*, 529.
(52) Liu, F.; Eisenberg, A. *J. Am. Chem. Soc.* **2003**, *125*, 15059.
(53) Hoppenbrouwers, E.; Li, Z.; Liu, G. *Macromolecules* **2003**, *36*, 876.
(54) Saito, R.; Fujita, A.; Ichimura, A.; Ishizu, K. *J. Polym. Sci., Part A: Polym. Chem.* **2000**, *38*, 2091.
(55) Erhardt, R.; Böker, A.; Zettl, H.; Kaya, H.; Pyckhout-Hintzen, W.; Krausch, G.; Abetz, V.; Müller, A. H. E. *Macromolecules* **2001**, *34*, 1069.
(56) Loo, Y.-L.; Register, R. A.; Ryan, A. J. *Macromolecules* **2002**, *35*, 2365.
(57) Quiram, D. J.; Register, R. A.; Marchand, G. R.; Adamson, D. H. *Macromolecules* **1998**, *31*, 4891.

MA060799K